Suv4-20h1 promotes G1 to S phase transition by downregulating p21$^{\text{WAF1/CIP1}}$ expression in chronic myeloid leukemia K562 cells

YUPENG WU[1,2*], YADONG WANG[1*], MING LIU[1], MIN NIE[1], YING WANG[1], YEXUAN DENG[1],
BING YAO[1], TAO GUI[1], XINYU LI[1], LINGLING MA[1], CHAN GUO[1], CHI MA[1], JUNYI JU[1] and QUAN ZHAO[1]

[1]The State Key Laboratory of Pharmaceutical Biotechnology, School of Life Sciences, Nanjing
University, Nanjing, Jiangsu 210023; [2]Anhui Research Institute for Family Planning, Anhui
Research Center for Population and Birth Control, Hefei, Anhui 230031, P.R. China

Abstract. Methylation of histone H4 lysine 20 (H4K20) has been associated with cancer. However, the functions of the histone methyltransferases that trigger histone H4K20 methylation in cancers, including suppressor of variegation 4-20 homolog 1 (Suv4-20h1), remain elusive. In the present study, it was demonstrated that the knockdown of the histone H4K20 methyltransferase Suv4-20h1 resulted in growth inhibition in chronic myeloid leukemia K562 cells. Disruption of Suv4-20h1 expression induced G_1 arrest in the cell cycle and increased expression levels of cyclin dependent kinase inhibitor 1A (p21$^{\text{WAF1/CIP1}}$), an essential cell cycle protein involved in checkpoint regulation. Chromatin immunoprecipitation analysis demonstrated that Suv4-20h1 directly binds to the promoter of the p21 gene and that methylation of histone H4K20 correlates with repression of p21 expression. Thus, these data suggest that Suv4-20h1 is important for the regulation of the cell cycle in K562 cells and may be a potential therapeutic target for leukemia.

Introduction

Histone lysine methylation induced by histone lysine methyltransferases (HMTs) play a critical role in epigenetic regulation of biological process, such as gene transcription, chromatin remodeling, DNA replication and recombination (1,2). On the N-terminal tail of histone H4, Lys 20 is the only lysine residue known to be methylated. In mammals, Set8/PR-Set7 catalyzes the monomethylation of H4K20, whereas Suv4-20h1

and Suv4-20h2 mediate the dimethylation and trimethylation of H4K20 (3,4). Disruption of these H4K20 methyltransferases results in genome instability, thus indicating their important roles in genome integrity maintenance (4,5). Whereas H4K20me2 is broadly distributed across the genome, H4K20me3 is enriched in constitutive heterochromatin, although H4K20me3 is not enriched at the promoters of inactive genes, as shown by ChIP analyses (3,6-9).

Aberrant histone H4K20 methylation has been associated with carcinogenesis and cancer progression in various cancers (10-12). Loss of histone H4K20me3 is considered a hallmark of cancers, including breast cancer, prostate cancer and lung cancer (10-12). However, there have been some recently observed discrepancies in the methylation status of histone H4K20 in some cancers, e.g., breast tumors. There have also been some conflicting reports in which the levels of H4K20me3 have been found to be increased (13). Furthermore, a recent study from a meta-analysis has identified that Suv4-20h1 is among the 8 (out of 50) dysregulated histone lysine methyltransferases in breast cancer induced by genetic alterations (14). Gain or amplification of Suv4-20h1 has also been observed in most breast cancer cell lines; therefore, Suv4-20h1 is highly expressed in these cancer cells compared with non-tumorigenic breast epithelial cells (14). In addition, studies in the TCGA database have demonstrated that Suv4-20h1 is also amplified in many types of human cancers, including breast, esophageal, bladder, and head and neck (15). The expression profiles of 11 squamous cell carcinoma cell lines have demonstrated that Suv4-20h1 is significantly highly expressed in these cells compared with normal keratinocytes (15). However, the functions of Suv4-20h1 in cancer remain unknown.

In the present study, we sought to characterize the role of Suv4-20h1 in leukemia K562 cells. We found that Suv4-20h1 accelerates the cell cycle G1/S transition and promotes leukemia K562 cell growth. The newly identified Suv4-20h1/p21 pathway plays a key role in the regulation of leukemia K562 cell proliferation.

Materials and methods

Plasmid construction. The full-length coding sequence (CDS) of the Suv4-20h1 was amplified from a K562 cDNA template

Correspondence to: Professor Quan Zhao or Dr Junyi Ju, The State Key Laboratory of Pharmaceutical Biotechnology, School of Life Sciences, Nanjing University, 163 Xianlin Avenue, Nanjing, Jiangsu 210023, P.R. China
E-mail: qzhao@nju.edu.cn
E-mail: jujunyi@nju.edu.cn

*Contributed equally

by polymerase chain reaction (PCR) using primer pairs with *EcoR* I/*Xho* I sites. The PCR products were digested with *EcoR* I/*Xho* I (New England Biolabs, MA, USA), inserted into the MSCV-3HA-IRES-HA vector, and confirmed by DNA sequencing.

Cell lines and cell culture. The human chronic myeloid leukemia cell line K562 and its derivatives SCR (stably transfected scrambled shRNA), Suv4-20h1 KD (stably transfected Suv4-20h1 shRNA), MSCV (stably transfected MSCV-3HA-IRES-GFP), and MSCV-Suv4-20h1FLC (stably transfected MSCV-3HA-IRES-GFP+Suv4-20h1 full length CDS) were established as previously described (16). Cells were maintained in gelatinized flasks in RPMI 1640 medium supplemented with 10% fetal bovine serum, 100 U penicillin/100 mg streptomycin (Gibco, Life Technologies, NY, USA) at 37°C and 5% CO_2.

Cell proliferation assay. The cell proliferation index was first analyzed using a hemocytometer. To accurately measure cell proliferation, the percentage of S-phase cells in the population was determined by using a Cell-Light™ EdU flow cytometry assay kit (Guangzhou RiboBio Co., Ltd., Guangzhou, China), according to the manufacturer's protocol (http://www.ribobio.com/sitecn/Product.aspx?id=93) for flow cytometry. EdU (5-ethynyl-2'-deoxyuridine) is a thymidine analog that is incorporated into DNA during active DNA synthesis. Newly synthesized DNA and total DNA were detected and quantified by flow cytometry with EdU and nuclear dyes. The original FACS data were imported and analyzed in WinMDI 2.9 software to obtain detailed values for the S-phase cells and all other cell populations. These values were entered into GraphPad Prism 5 (GraphPad Software, Inc., La Jolla, CA, USA), and then a cell proliferation histogram was generated.

Apoptosis assay. Cells were collected and washed twice in phosphate-buffered saline (PBS). Then, the apoptotic and dead cells were detected with an Annexin V-APC/7-AAD Apoptosis Detection kit (KeyGEN Biotech, Nanjing, China) according to the manufacturer's instructions. Data were collected using a BD FACSCalibur Flow Cytometer. The original FACS data were imported and analyzed in Flowjo.7.6.1 software (Tree Star, Inc. Ashland, OR, USA) to acquire detailed values for the different stages of the K562 derivative cells. These values were entered into GraphPad Prism 5, and then an apoptosis histogram was generated.

Cell cycle assay. Cells were collected, washed in PBS, and fixed and permeabilized in 70% ethanol. For determination of DNA content, the cells were stained with a Cell Cycle Detection Kit (KeyGEN Biotech) according to the manufacturer's instructions. Data were collected using a BD FACSCalibur Flow Cytometer. For each sample, 20,000 events were collected, and aggregated cells were gated out. The original FACS data were imported and analyzed through ModFit LT 3.2 software to acquire the detailed values for the different phases of the cell cycle. These values were entered into GraphPad Prism 5, and a cell cycle histogram was generated.

Quantitative RT-PCR. Total RNA was isolated from cells with TRIzol reagent (Invitrogen, Carlsbad, CA, USA). cDNA was generated using PrimeScript™ RT Master Mix (Perfect Real Time) kit (Takara Bio, Otsu, Japan). Quantitative reverse-transcriptase PCR (qRT-PCR) primers were selected from the PrimerBank (http://pga.mgh.harvard.edu/primerbank/) or designed online on the Primer3 website: http://bioinfo.ut.ee/primer3-0.4.0/primer3/. qRT-PCR was performed using FastStart Universal SYBR-Green Master (Rox) (Roche, South San Francisco, CA) in a final volume of 20 μl in a Rotorgene 2000 (Corbett Research). Relative quantification was performed for several potential target genes using GAPDH as an internal reference. Each reaction was performed in triplicate. The primers used are listed in Table I. Student's t-tests were used to derive the significance of the differences between mean values.

Western blot analysis. Western blot analysis of the cellular extracts was performed as previously described (16). The specific primary antibodies used in this study were as follows: Mouse anti-HA monoclonal antibody (12CA5; Roche), mouse anti-GAPDH monoclonal antibody (sc-47724; Santa Cruz, Biotechnology, Inc., Santa Cruz, CA), rabbit anti-p21$^{Waf1/Cip1}$ antibody (12D1; CST, Beverly, MA, USA), mouse anti-p53 antibody (1C12; CST), rabbit anti-PTEN antibody (ab170941; Abcam, Cambridge, MA, USA), rabbit anti-p27 antibody (ab32034; Abcam), mouse anti-E2F1 antibody (05-379; Millipore Billerica, MA, USA), and rabbit anti-CCND1 antibody (ab134175; Abcam).

Chromatin immunoprecipitation (ChIP). ChIP assays were performed by using standard ChIP procedures as previously described (17). Chromatin fractions from K562 cell derivatives were immunoprecipitated with specific antibodies. Normal rabbit immunoglobulin G (IgG) served as the control. The antibodies used were as follows: Anti-rabbit IgG (A7028 and A7016; Beyotime Biotech, Jiangsu, China), anti-HA (12CA5, Roche, South San Francisco, CA, USA), anti-H4K20me2 (07-367, Millipore), and anti-H4K20me3 (ab9053, Abcam). Q-PCR was performed using FastStart Universal SYBR-Green Master mix (Rox) (Roche) in a Rotorgene 2000 instrument (Corbett Research), using immunoprecipitated gDNA. The detailed values were entered into Origin 7.5, and the relative enrichment of ChIP DNA was calculated relative to the input DNA. Each experiment was performed at least twice independently. The primers used are listed in Table II. Student's t-tests were used to derive the significance of the differences between mean values.

Results

Suv4-20h1 promotes K562 cell proliferation. To characterize the function of Suv4-20h1 in K562 cells, we generated a stable Suv4-20h1 knockdown K562 cell line (Suv4-20h1KD) by using a lentiviral vector containing specific shRNA. Quantitative real-time PCR confirmed that the expression levels of Suv4-20h1 were decreased to ~75% of the scrambled control (SCR) (Fig. 1A). Unfortunately, we were unable to perform western blot analysis to verify the protein level of Suv4-20h1, owing to the current lack of commercially available human-specific anti-Suv4-20h1 antibodies. Consequently,

Table I. Quantitative RT-PCR primer sequences.

Gene	5' Primer	3' Primer
CCND1	ACCTTCCGCAGTGCTCCTA	CCCAGCCAAGAAACGGTCC
CCND2	GGTGGTGCTGGGGAAGTTGAAGTG	TCGACGGTGGGTACATGGCAAACT
CCNB1	AGATTGGAGAGGTTGATGTC	CGATGTGGCATACTTGTTC
CCNE1	AACTGTGTCAAGTGGATGG	CTGCTTCTTACCGCTCTG
CDK6	CTTCATTCACACCGAGTAGT	TGGACTGGAGCAAGACTT
p27	GGAGCAATGCGCAGGAATAA	TGGGGAACCGTCTGAAACAT
p21	CTGGAGACTCTCAGGGTCGAAA	GATTAGGGCTTCCTCTTGGAGAA
p53	GAGGTTGGCTCTGACTGTACC	TCCGTCCCAGTAGATTACCAC
p57	ACGATGGAGCGTCTTGTC	CCTGCTGGAAGTCGTAATC
PTEN	TGGATTCGACTTAGACTTGACCT	GGTGGGTTATGGTCTTCAAAAGG
E2F1	AGCTGGACCACCTGATGAAT	GAGGGGCTTTGATCACCATA
SMYD5	CCAGCAGCTGCAGCCTCAAAAT	TGCCGGTGATATTCTGCTCCCCAA
Suv4-20h1	GAATACTAGCGCCTTTCCTTCG	GCCCATTCGCCTGAAGTCAA
GAPDH	TGTTGCCATCAATGACCCCTT	CTCCACGACGTACTCAGCG

Table II. ChIP primer sequences.

Locus	5' Primer	3' Primer
p21 pro	CATTTGACAACCAGCCCTTT	TGGGAGGACACAGTAGCAGA
E2F1 pro	CGTTGGCTGTTGGAGATTTT	TTGCCTCACCCATGACATTA

we observed a significant decrease in the growth rate of the Suv4-20h1 KD cells compared with the SCR cells (Fig. 1B). To measure the cell proliferation rate, Cell-Light™ EdU flow cytometry assays were used to quantify the percentage of S-phase cells in the total cell population. The results show a separation of proliferating cells which have incorporated EdU and non-proliferating cells which have not. We observed fewer proliferative cells in the Suv4-20h1 knockdown cell population than in the SCR cell population (Fig. 1C).

To complement the Suv4-20h1 knockdown cells, we generated a stable Suv4-20h1 overexpression K562 cell line by using a retrovirus vector (MSCV-3HA-IRES-GFP) containing the full-length Suv4-20h1 CDS. Quantitative real-time PCR revealed that levels of Suv4-20h1 in the MSCV-Suv4-20h1FLC cells were approximately 3-fold higher than those in the MSCV vector-alone control cells (Fig. 1D). Western blot analysis with anti-HA antibodies confirmed the presence of the exogenously expressed HA-tagged Suv4-20h1 (Fig. 1D). We found that overexpression of Suv4-20h1 significantly increased the proliferative cell population during the cell cycle (Fig. 1E), thus further confirming that Suv4-20h1 plays a crucial role in promoting leukemia K562 cell proliferation.

Knockdown of Suv4-20h1 induces G1/S cell cycle arrest. To investigate the effect of Suv4-20h1 on cell cycle progression, we performed flow cytometric analysis of the cellular DNA content in K562 cells. We observed more Suv4-20h1 KD cells in G1 phase compared with SCR cells, which was

accompanied by a decrease in the number of cells in S phase in the cell cycle (Fig. 2A). In contrast, fewer cells overexpressing Suv4-20h1FLC were in G1 phase, as compared with the control cells with MSCV alone, whereas more cells overexpressing Suv4-20h1FLC were in S phase, as compared with the control cells with MSCV alone (Fig. 2B). Our results indicated that knockdown of Suv4-20h1 induces G1-S cell cycle arrest.

Next, we determined whether Suv4-20h1 plays a role in cell apoptosis. The total cell apoptosis rate was evaluated by flow cytometric analysis after double staining with 7-AAD and Annexin V-APC in which apoptotic cells (positive for Annexin V-APC) are distinguishable from viable cells (negative for Annexin V-APC and 7-AAD). We found no changes in the apoptotic cell populations between Suv4-20h1 KD cells and SCR cells (Fig. 2C). Suv4-20h1-overexpressing cells and MSCV control cells also displayed a similar pattern of apoptosis (Fig. 2D). In Fig. 2C and D, there is no difference (P>0.05) between tested groups and corresponding controls, including Normal cells, Early apoptotic cells, Late apoptotic cells and Dead cells. Thus, Suv4-20h1 has no effect on cell apoptosis in K562 cells, suggesting that Suv4-20h1 promotes cell growth is not due to less dead cells occurred, rather a faster proliferation of cells as demonstrated by the EdU assays.

Suv4-20h1 represses p21 expression in K562 cells. To understand the mechanism underlying the G1/S phase arrest in Suv4-20h1 knockdown cells, we next examined the effect of Suv4-20h1 on various key cell cycle regulatory proteins in the G1 phase of the cell cycle, including CCND1, CCND2,
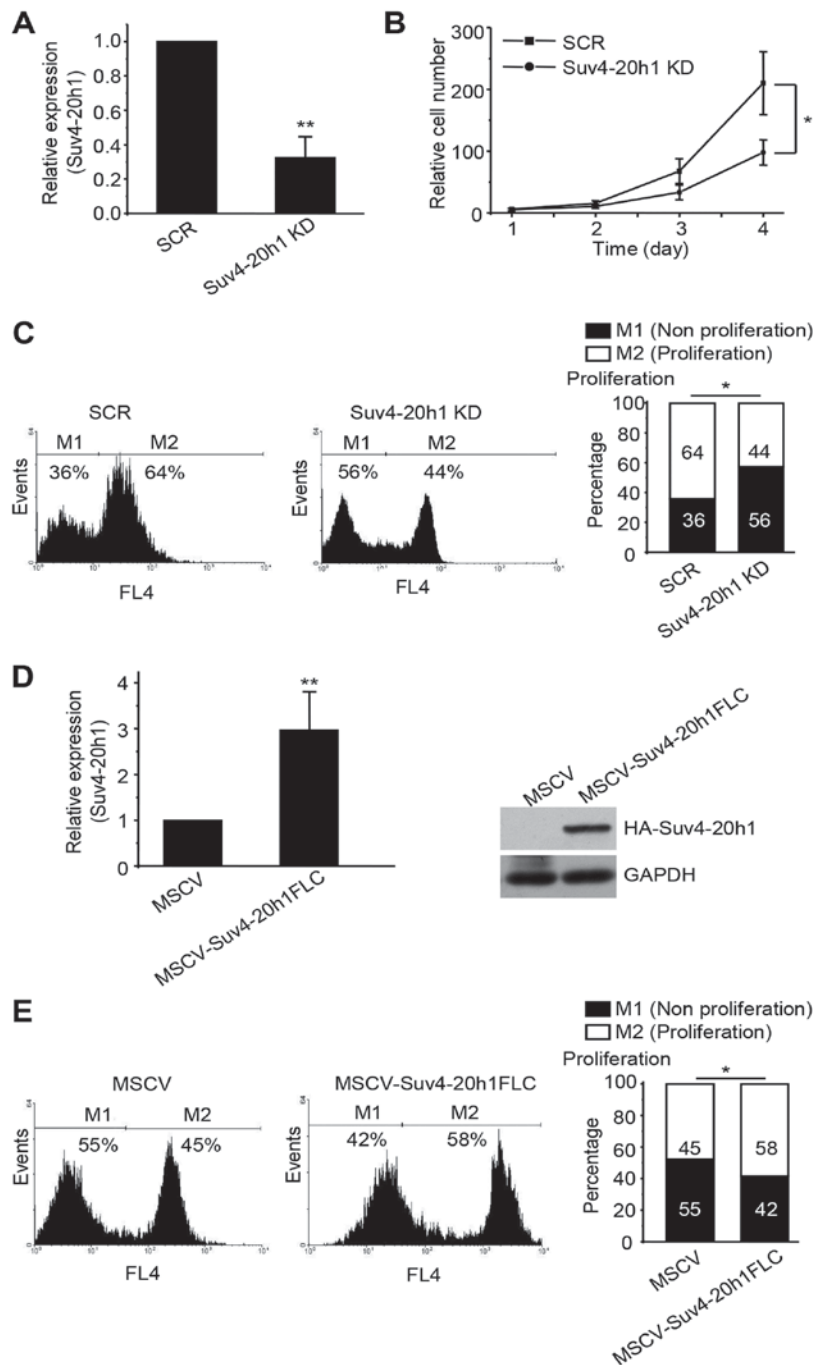
Figure 1. Suv4-20h1 promotes K562 cell proliferation. (A) Quantitative real-time PCR analysis of Suv4-20h1 from SCR or Suv4-20h1 KD cells. Data are normalized to GAPDH mRNA levels. The results are shown as the mean ± SD from three independent experiments; **P<0.01 compared with SCR. (B) Growth curves of the SCR and Suv4-20h1 KD cells. The results are shown as the means ± SD from three independent experiments; *P<0.05 compared with the corresponding control. (C) The proliferation of SCR and Suv4-20h1 KD cells was measured with Cell-Light™ EdU and flow cytometry. The original FACS data were transformed into a set of histograms with WinMDI 2.9 and GraphPad Prism 5 software. The results are shown as the means ± SD from three independent experiments; *P<0.05 compared with the corresponding control. (D) Suv4-20h1 gene expression analysis of MSCV or MSCV-Suv4-20h1FLC cells by quantitative real-time PCR of RNA and western blotting with the indicated antibodies. The results are shown as the mean ± SD (n=3), **P<0.01. (E) The proliferation of MSCV and MSCV-Suv4-20h1FLC cells was measured by using Cell-Light™ EdU and flow cytometry. The original FACS data were transformed into a set of histograms with WinMDI 2.9 and GraphPad Prism 5 software. The results are shown as the means ± SD from three independent experiments; *P<0.05 compared with the corresponding control.

CCNB1, CCNE1, CDK6, p27, p21, p57, p53, PTEN, E2F1, and SMYD5 (18,19). Quantitative real-time PCR demonstrated that the expression level of p21 was most increased in Suv4-20h1 KD cells compared with the SCR cells (Fig. 3A). In contrast, we did not observe significant changes in the expression levels of any other key molecules, such as p53

and PTEN. The effect of Suv4-20h1 on p21 expression was further confirmed at the protein level by western blotting. The levels of p21 protein were significantly increased in the Suv4-20h1 knockdown k562 cells (Fig. 3B) compared with controls, thereby confirming that Suv4-20h1 represses p21 expression.
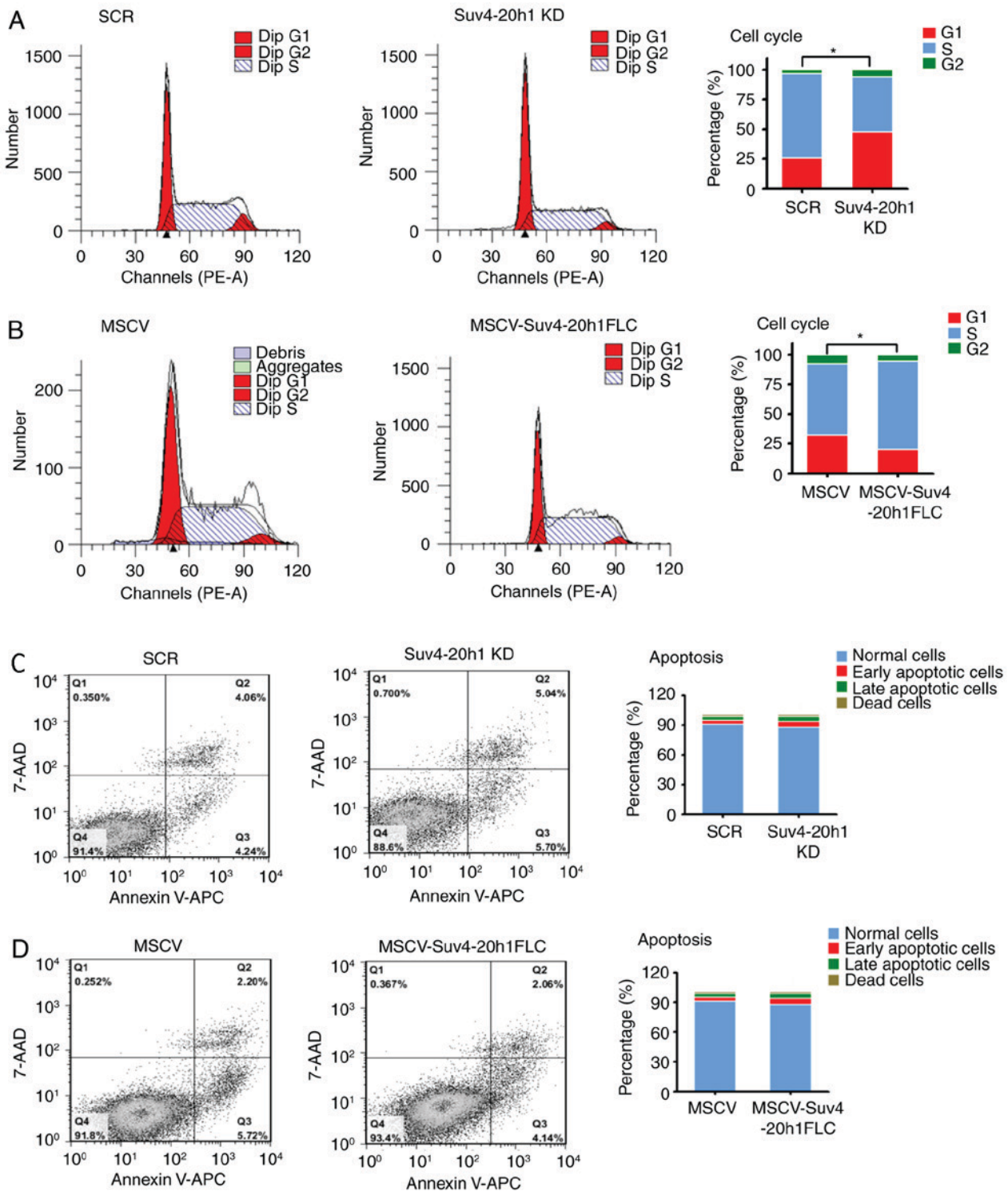
Figure 2. Knockdown of Suv4-20h1 induces G1/S cell cycle arrest. (A) The cell cycle phase of SCR or Suv4-20h1 KD cells was determined by using flow cytometry. The original FACS data were entered into and analyzed with ModFit LT 3.2 software and transformed into a histogram with GraphPad Prism 5 software. The results are shown as the means ± SD from three independent experiments; *P<0.05 compared with the corresponding control. (B) The cell cycle phase of MSCV or MSCV-Suv4-20h1FLC cells was determined by flow cytometry. The original FACS data were entered into and analyzed with ModFit LT 3.2 software and transformed into a histogram with GraphPad Prism 5 software. The results are shown as the means ± SD from three independent experiments; *P<0.05 compared with the corresponding control. (C) The apoptosis of SCR or Suv4-20h1 KD cells was analyzed with flow cytometry. The percentages of cells in different states were quantified using Flowjo.7.6.1 software, and histograms were generated in GraphPad Prism 5. The results are shown as the means ± SD from three independent experiments. (D) The apoptosis of MSCV or MSCV-Suv4-20h1FLC cells was analyzed with flow cytometry. The percentages of cells in different states were quantified using Flowjo.7.6.1 software, and histograms were generated in GraphPad Prism 5. The results are shown as the means ± SD from three independent experiments.

Suv4-20h1 binds the p21 promoter. To examine whether Suv4-20h1 directly regulates p21, we performed ChIP assays using antibodies against HA in K562 cells stably overexpressing Suv4-20h1. We found that HA-tagged Suv4-20h1 was
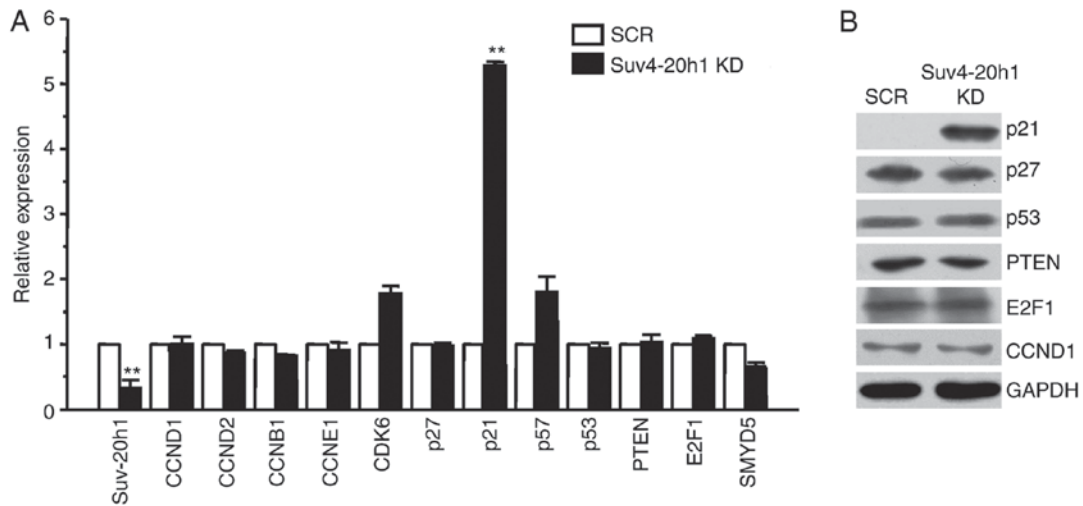
Figure 3. Suv4-20h1 represses p21 expression in K562 cells. (A) Suv4-20h1, CCND1, CCND2, CCNB1, CCNE1, CDK6, p27, p21, p57, p53, PTEN, E2F1 and SMYD5 gene expression analysis by qRT-PCR of RNA extracted from SCR and Suv4-20h1 KD cells. Data are normalized to GAPDH mRNA. The results are shown as the mean ± SD from three independent experiments; **P<0.01 compared with SCR. (B) Western blot analysis of cellular extracts from SCR and Suv4-20h1 KD K562 cells, detected with the indicated antibodies. GAPDH is a loading control.
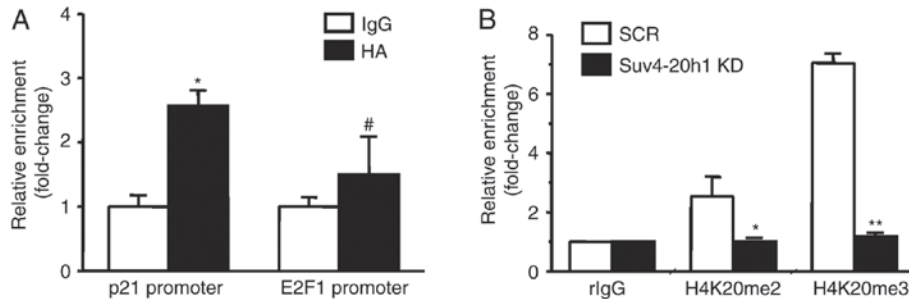

Figure 4. Suv4-20h1 binds the p21 promoter. (A) ChIP analysis of Suv4-20h1 in the p21 and E2F1 promoter, in anti-HA in MSCV-Suv4-20h1FLC cells. Rabbit IgG served as the control. The results are shown as the mean ± SD of three independent experiments. $^{#}$P>0.05, *P<0.05 compared with IgG control. (B) Histone H4K20me2 and H4K20me3 ChIP analyses of the p21 promoter were performed on SCR and Suv4-20h1 KD K562 cells. The results are shown as the mean ± SD of three independent experiments. *P<0.05, **P<0.01 compared with the SCR control.

significantly enriched at the p21 promoter, as compared with the IgG control. HA-tagged Suv4-20h1 was not enriched in the E2F1 promoter, a result consistent with our previous E2F1 expression results (Fig. 4A).

Suv4-20h1 triggers histone H4K20me2/3 activity. To examine whether Suv4-20h1 affects the histones at the p21 promoter region, we performed ChIP analysis using antibodies against H4K20me2 and H4K20me3. We found that enrichment of histones H4K20me2 and H4K20me3 at the p21 promoter was significantly decreased in Suv4-20h1 KD cells compared with SCR cells (Fig. 4B). These results indicated that Suv4-20h1 represses p21 expression via methylation of histone H4K20.

Discussion

In this study, we sought to investigate the role of Suv4-20h1 in leukemia K562 cells. We found that knockdown of Suv4-20h1 resulted in growth inhibition of leukemia K562 cells through inducing G1 arrest during the cell cycle. A key cell cycle-related gene, p21, was identified to be a downstream target of Suv4-20h1 repression. These results demonstrated
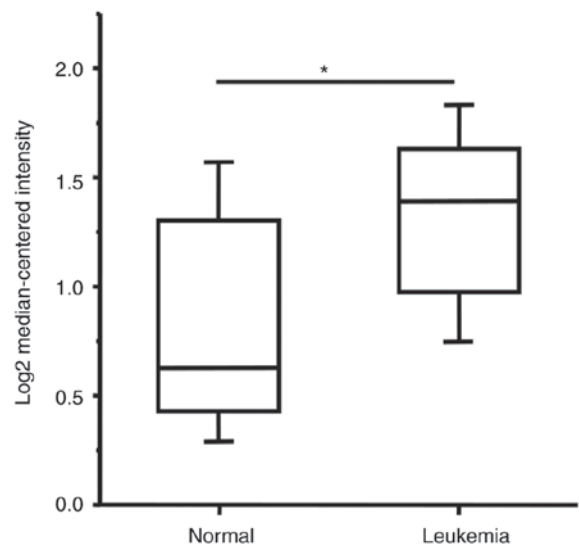

Figure 5. Suv4-20h1 is highly upregulated in leukemia patients (n=2022) compared with non-leukemia and healthy controls (n=74). The gene expression data were obtained from Oncomine database (www.oncomine.org), and the original data were acquired from GEO database with the accession number GSE13159. The results are shown as the log2 median-centered intensity. *P<0.05 compared with the normal controls.

that Suv4-20h1 is a potentially oncogenic protein. In fact, we have examined a deposited high-throughput database ONCOMINE (https://www.oncomine.org) and found that the expression levels of Suv4-20h1 are indeed significantly higher in leukemia patients (combined different kinds of leukemia from the reference) than normal controls (Fig. 5). Similarly, we searched some databases such as TCGA (https://cancergenome.nih.gov/) and R2 platform (http://r2.amc.nl), but could not find related data regarding the expression of Suv4-20h1 in the context of clinical parameters such as Overall Survival (OS), Relapse Free Survival (RFS).

The cell cycle has been shown to be associated with the methylation state of histone H4K20 (3,11). The balance of H4K20 methylation is important in the transition from cell proliferation to differentiation (3). Among the different methylation states of H4K20 in the cell cycle, H4K20me1 is the most dynamic, whereas H4K20me3 is the least abundant and undergoes only modest changes during the cell cycle (20,21). In proliferating cells, H4K20me2 is the most abundant form of methylation, which occurs in 80% of all histone H4 tails (4,20). In mouse embryonic fibroblast cells, Suv4-20h1 preferentially induces H4K20me2, and this induction may partially account for the role of Suv4-20h1 in cell proliferation (4). In fact, in an analysis of mouse embryonic fibroblasts (MEFs) derived from Suv4-20h1/h2 double knockout mice (Suv4-20h-dn), a decrease in S-phase cells with a concomitant increase in G1-phase cells has been shown, as compared with MEFs derived from wild-type mice, thus indicating a partial block in the G1/S transition (4). Consistently with these results, we found that Suv4-20h1 methylates histone H4 at both H4K20me2 and H4K20me3 in leukemia K562 cells, and knockdown of Suv4-20h1 caused G1/S stage cell cycle arrest, thus suggesting that Suv4-20h1 may be one of the major cell cycle regulators. A similar scenario occurs in head and neck squamous carcinoma cells in which siRNA-medicated Suv4-20h1 knockdown induces a significant decrease in the proportion of cells at the S phase with concomitantly more cells at the G1 phase (15).

Cell cycle progression is precisely regulated by a series of cell cycle regulators, including cyclins, cyclin-dependent kinases (CDKs), and CDK inhibitors (CDKIs) (22-24). p21 is a member of the CDKI family, which comprises kinase inhibitor proteins or CDK-interacting proteins, and it inhibits the activity of cyclins at the G1 checkpoint and influences the transition of cells from the G1 phase to the S phase of the cell cycle (18,24). In this study, we found that knockdown of Suv4-20h1 significantly increased p21 expression. Interestingly, we did not observe any changes in p27 and p57, the two other kinase inhibitor proteins, after knockdown of Suv4-20h1, thus suggesting the regulatory specificity of Suv4-20h1 for p21. Therefore, our results indicated that Suv4-20h1 represses p21 expression and consequently prevents inhibition of cyclins at the G1 checkpoint, thus promoting the G1/S transition.

Proper regulation of Suv4-20 h proteins and dynamic control of H4K20 methylation throughout the cell cycle is of great importance to maintain cellular homeostasis (4,20). Whereas loss of H4K20me3 has been regarded as a potential hallmark of human cancer, these observations have also been inconsistent, with some reports of increased Suv4-20h1 expression (13-15). There are three possible explanations for this discrepancy. First, the precise regulation of histone H4K20 methylation by Set8/PR-Set7, Suv4-20h1 and Suv4-20h2 may be balanced for proper cell cycle progression. A Change in one enzyme may not alter the cellular or local gene histone H4K20 methylation levels in different contexts. Second, Suv4-20h1 may target other proteins for methylation/interaction, an effect that may later play a role in the cell cycle; for example, Suv4-20h1 enhances the phosphorylation and transcription of ERK1 in cancer cells, thereby promoting cancer cell proliferation (15). Third, some discrepancies may be due to differences in the genetic backgrounds or progressive stages of the cells or specimens. Therefore, careful analyses are required to determine the relationship between Suv4-20h1 expression and histone H4K20 methylation status in different contexts.

In conclusion, our data demonstrated that Suv4-20h1 represses p21 expression to accelerate the G1/S transition during the cell cycle in human leukemia K562 cells. These data suggested that Suv4-20h1 plays an important role in cancer cell proliferation. Given that Suv4-20h1 is frequently overexpressed in various types of cancers, inhibition of Suv4-20h1 may be an alternative therapeutic strategy for cancer patients exhibiting this overexpression.

Acknowledgements

References

1. Greer EL and Shi Y: Histone methylation: A dynamic mark in health, disease and inheritance. Nat Rev Genet 13: 343-357, 2012.
2. Chi P, Allis CD and Wang GG: Covalent histone modifications-miswritten, misinterpreted and mis-erased in human cancers. Nat Rev Genet 10: 457-469, 2010.
3. Jorgensen S, Schotta G and Sørensen CS: Histone H4 lysine 20 methylation: Key player in epigenetic regulation of genomic integrity. Nat Rev Genet 41: 2797-2806, 2013.
4. Schotta G, Sengupta R, Kubicek S, Malin S, Kauer M, Callén E, Celeste A, Pagani M, Opravil S, De La Rosa-Velazquez IA, et al: A chromatin-wide transition to H4K20 monomethylation impairs genome integrity and programmed DNA rearrangements in the mouse. Genes Dev 22: 2048-2061, 2008.
5. Schotta G, Lachner M, Sarma K, Ebert A, Sengupta R, Reuter G, Reinberg D and Jenuwein T: A silencing pathway to induce H3-K9 and H4-K20 trimethylation at constitutive heterochromatin. Genes Dev 18: 1251-1262, 2004.
6. Kohlmaier A, Savarese F, Lachner M, Martens J, Jenuwein T and Wutz A: A chromosomal memory triggered by Xist regulates histone methylation in X inactivation. PLoS Biol 2: E171, 2004.
7. Sims JK, Houston SI, Magazinnik T and Rice JC: A trans-tail histone code defined by monomethylated H4 Lys-20 and H3 Lys-9 demarcates distinct regions of silent chromatin. J Biol Chem 281: 12760-12766, 2006.
8. Barski A, Cuddapah S, Cui K, Roh TY, Schones DE, Wang Z, Wei G, Chepelev I and Zhao K: High-resolution profiling of histone methylations in the human genome. Cell 129: 823-837, 2007.
9. Mikkelsen TS, Ku M, Jaffe DB, Issac B, Lieberman E, Giannoukos G, Alvarez P, Brockman W, Kim TK, Koche RP, et al: Genome-wide maps of chromatin state in pluripotent and lineage-committed cells. Nature 448: 553-560, 2007.
10. Fraga MF, Ballestar E, Villar-Garea A, Boix-Chornet M, Espada J, Schotta G, Bonaldi T, Haydon C, Ropero S, Petrie K, et al: Loss of acetylation at Lys16 and trimethylation at Lys20 of histone H4 is a common hallmark of human cancer. Nat Genet 37: 391-400, 2005.

11. Balakrishnan L and Milavetz B: Decoding the histone H4 lysine 20 methylation mark. Crit Rev Biochem Mol Biol 45: 440-452, 2010.

12. Van Den Broeck A, Brambilla E, Moro-Sibilot D, Lantuejoul S, Brambilla C, Eymin B, Khochbin S and Gazzeri S: Loss of histone H4K20 trimethylation occurs in preneoplasia and influences prognosis of non-small cell lung cancer. Clin Cancer Res 14: 7237-7245, 2008.

13. Elsheikh SE, Green AR, Rakha EA, Powe DG, Ahmed RA, Collins HM, Soria D, Garibaldi JM, Paish CE, Ammar AA, *et al*: Global histone modifications in breast cancer correlate with tumor phenotypes, prognostic factors and patient outcome. Cancer Res 69: 3802-3809, 2009.

14. Liu L, Kimball S, Liu H, Holowatyj A and Yang ZQ: Genetic alterations of histone lysine methyltransferases and their significance in breast cancer. Oncotarget 6: 2466-2482, 2015.

15. Vougiouklakis T, Sone K, Saloura V, Cho HS, Suzuki T, Dohmae N, Alachkar H, Nakamura Y and Hamamoto R: SUV420H1 enhances the phosphorylation and transcription of ERK1 in cancer cells. Oncotarget 6: 43162-43171, 2015.

16. Rank G, Cerruti L, Simpson RJ, Moritz RL, Jane SM and Zhao Q: Identification of a PRMT5-dependent repressor complex linked to silencing of human fetal globin gene expression. Blood 116: 1585-1592, 2010.

17. Zhao Q, Rank G, Tan YT, Li H, Moritz RL, Simpson RJ, Cerruti L, Curtis DJ, Patel DJ, Allis CD, *et al*: PRMT5-mediated methylation of histone H4R3 recruits DNMT3A, coupling histone and DNA methylation in gene silencing. Nat Struct Mol Biol 16: 304-311, 2009.

18. Kreis NN, Louwen F and Yuan J: Less understood issues: p21(Cip1) in mitosis and its therapeutic potential. Oncogene 34: 1758-1767, 2015.

19. Tanaka T and Iino M: Knockdown of Sec8 promotes cell-cycle arrest at G1/S phase by inducing p21 via control of FOXO proteins. FEBS J 281: 1068-1084, 2014.

20. Pesavento JJ, Yang H, Kelleher NL and Mizzen CA: Certain and progressive methylation of histone H4 at lysine 20 during the cell cycle. Mol Cell Biol 28: 468-486, 2008.

21. Tsang LW, Hu N and Underhill DA: Comparative analyses of SUV420H1 isoforms and SUV420H2 reveal differences in their cellular localization and effects on myogenic differentiation. PLoS One 5: e14447, 2010.

22. Lim S and Kaldis P: Cdks, cyclins and CKIs: Roles beyond cell cycle regulation. Development 140: 3079-3093, 2013.

23. Malumbres M and Barbacid M: Cell cycle, CDKs and cancer: A changing paradigm. Nat Rev Cancer 9: 153-166, 2009.

24. Bertoli C, Skotheim JM and de Bruin RA: Control of cell cycle transcription during G1 and S phases. Nat Rev Mol Cell Biol 14: 518-528, 2013.